On-chip wireless optical communication through plasmonic nanoantennas

On-chip Wireless Optical Communication Through Plasmonic Nanoantennas

Giovanna Calò [1], Gaetano Bellanca[2], Ali Emre Kaplan[2], Franco Fuschini[3],
Marina Barbiroli[3], Michele Bozzetti [1], Paolo Bassi[3] and Vincenzo Petruzzelli[1]
[1]Dipartimento di Ingegneria Elettrica e dell'Informazione, Politecnico di Bari, Via Orabona, 4, Bari, 70125, Italy,
giovanna.calo@poliba.it
[2]Department of Engineering, University of Ferrara, Via Saragat, 1, Ferrara, 44122, Italy
[3]Department of Electrical, Electronic and Information Engineering, University of Bologna, Viale del Risorgimento, 2,
Bologna, 40136, Italy

***Abstract*—On-chip wireless optical communications among distant cores in chip multiprocessors can lead to a completely new approach to overcome the limits of current on-chip communication. In fact, using wireless connections mitigates the problems related to the design and the fabrication of hugely complex switching fabrics, where long paths suffer of crosstalk and loss issues. Implementing wireless communication at optical frequencies allows simplifications in network design and management. In this paper, a solution based on Vivaldi plasmonic antennas integrated with silicon waveguides is presented. Moreover, on-chip wireless propagation characteristics and point-to-point link performances in homogeneous and multilayered medium are investigated and discussed.**

***Index Terms*—Optical antennas, Nano antennas, Nanophotonics, Surface plasmons, Wireless optical communications, Optical networks on chip.**

I. Introduction

The interconnection and the communication between the cores of Chip Multiprocessors (CMPs) is a major challenge, especially when the number of cores increases toward kilo-core architectures. In this context, traditional point-to-point connections through dedicated wires, based on planar metal interconnects, cannot meet the requirements of high bandwidth, low-power and low-latency. The most assessed technology to overcome these limitations exploits Network-on-chips (NoCs) [1] where communication lines are shared and the data traffic is ruled by switching elements, network interfaces and inter-switch links. However, a major limit of this technology arises from multi-hop communications and to the consequent high latency and power consumption.

Optical Network-on-Chip (ONoC) is a promising chip-scale optical communication technology with high bandwidth capacity and energy efficiency which can be profitably used to overcome these limitations [2]- [3]. With this approach, the communication between the different cores is made through a dedicated optical layer, thus exploiting the advantages of optical domain signal transmission such as high bandwidth and bitrate transparency. However, as the size of the optical network scales up, the complexity of the layout and of the routing scheme considerably increases and the overall power budget is strongly worsened by signal losses and crosstalk, due to waveguide crossings [5]- [6].

A new emerging approach to optical on-chip communication is the wireless transmission of optical signals exploiting dielectric or plasmonic nanoantennas [7]- [11]. Thanks to wireless connection among the furthest cores, Wireless Optical Networks on Chip (WONoC) can improve latency issues, alleviate topological constraints, and allow single-hop data transmission. Moreover, the integration of optical antennas with Silicon on Insulator (SOI) waveguides allows hybrid wired/wireless communication schemes and opens up new scenarios for network design and optimization.

The efficient coupling between plasmonic radiators and standard silicon waveguides is non-trivial and requires accurate design, especially when highly directive radiation is needed for point-to-point connections [12]- [16]. In [17] the authors proposed a Vivaldi antenna coupled to a silicon waveguide, in which efficient power transfer to the antenna is achieved by an hybrid Si-plasmonic coupler. This structure guarantees highly directive in-plane radiation and full compatibility with standard optical components in SOI technology.

In addition to the optimal design of the radiating elements, a topic that needs further investigations is the electromagnetic propagation in an on-chip environment [18]. In this case, the propagation conditions may strongly differ from the usual ones, where obstacles are localized and introduce basically diffraction phenomena. Here, the presence of multiple layers can also introduce waveguiding phenomena which can strongly influence the propagation.

In order to design wireless optical networks, it is advisable to develop propagation models (e.g. ray tracing models) which account for the propagation channel characteristics and for the physical environment properties, in analogy with radiofrequency and microwave wireless propagation. The development of reliable models describing the channel usually requires the comparison with on-site measurements. However, in the case of on-chip wireless connections at optical frequencies, such measurements are not yet available. Therefore, comparisons with three-dimensional full-wave simulations are required.

Based on the results of [17], in this paper we propose the analysis of the electromagnetic propagation in a point-to-point link between two Vivaldi antennas coupled to silicon waveguides

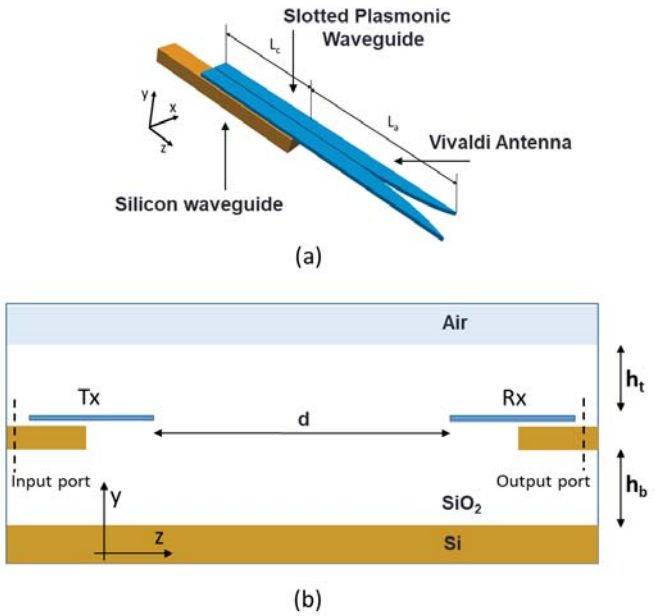

Fig. 1: Sketch of the Vivaldi antenna coupled to the Si waveguide (a) and of the link in a multilayered medium (b).

in different configurations. In particular, the electromagnetic propagation in homogeneous medium and in multilayered environment are considered. The results are obtained by three-dimensional Finite Difference Time Domain (FDTD) models [19] and they can be a first reference for the development of propagation channel models and ray-tracing algorithms.

II. Integrated Si-waveguide fed Vivaldi antenna for Optical Wireless Links

Fig.1 (a) shows the sketch of the Vivaldi antenna fed by a silicon waveguide. The optical signal is launched into the Si wire and it is vertically coupled to a plasmonic slotted waveguide, made of silver. The plasmonic slotted waveguide opens up into a Vivaldi antenna and radiates the signal in the surrounding medium, i.e. SiO_2. In the coupling section, the Si and the Ag structures are vertically separated by a gap $g = 80\ nm$. The width and the height of the Si wire are, respectively, $w = 380\ nm$ and $h = 220\ nm$, whereas the plasmonic waveguide width and the slot width are, respectively, $p = 270\ nm$ and $s = 30\ nm$. The thickness of the Ag layer is $t = 50\ nm$.

The length of the hybrid Si-plasmonic coupler, $L_c = 1.63\ \mu m$, was designed by applying the coupled mode theory (CMT) and the normal mode analysis [20], [21] and by validating and optimizing the design through three-dimensional Finite Element Method (FEM) simulations [22]. After designing the coupling section, the Vivaldi antenna width is constrained by the slotted waveguide width. The Vivaldi aperture profile is given by the following equations:

$$x = c_1 e^{Rz} + c_2 \tag{1}$$

with

$$c_1 = \frac{x_2 - x_1}{e^{Rz_2} - e^{Rz_1}} \tag{2}$$

and

$$c_2 = \frac{x_1 e^{Rz_2} - x_2 e^{Rz_1}}{e^{Rz_2} - e^{Rz_1}} \tag{3}$$

where R is the opening rate coefficient, x_1 and x_2 are the minimum and the maximum x coordinates of the Vivaldi profile and, similarly, z_1 and z_2 are the minimum and the maximum z coordinates. The antenna behavior was, therefore, optimized by varying the antenna length L_a. The optimal length value $L_a = 1.75\ \mu m$, corresponding to the maximum antenna gain $G = 9.9\ dB$, was found by FDTD simulations [19]. Further details on the coupler and on the antenna design and performance can be found in [17].

III. Optical wireless link between Si-waveguide fed Vivaldi antennas

Fig.1 (b) shows the sketch of the analyzed wireless link. The two Vivaldi antennas, coupled to Si waveguides and buried into SiO_2, are separated by a distance d. Moreover, different material layers are considered, as in typical SOI fabricated samples. In particular, an air over-layer and an Si substrate are sketched in Fig.1 (b). In the following, we will report the FDTD simulation results obtained by considering different scenarios derived from the scheme of Fig.1 (b). We will consider the simulation of the wireless link in a homogeneous medium (i.e. SiO_2 without both the air and the Si top and bottom layers, labeled as configuration (a) in the following) and then in a multilayer medium. In particular, in the multilayer case, we will consider three scenarios: 1) SiO_2 with an on-top air layer (configuration (b)), 2) SiO_2 with an on-bottom Si layer (configuration (c)), and 3) stacked Si, SiO_2, and air layers (configuration (d)). In all the analyzed cases, Perfectly Matched Layer (PML) boundary conditions are implemented to delimit the calculation domain. The three scenarios are the simplest models of the different topologies that one can find when realizing the real circuits, as mentioned before.

Fig.2 shows the electric field intensity (in logarithmic scale and in the YZ vertical plane) for the four above mentioned scenarios. In these simulations, only the transmitting antenna is considered. The top interface is located at a distance $h_t = 1.3\ \mu m$ from the antenna plane. The simulated wavelength is $\lambda = 1.55\ \mu m$. The bottom interface is instead positioned at $h_b = 1.0\ \mu m$ from the waveguide plane (see Fig.1 (b) for more details on the position of the two interfaces). As it can be observed, while in the homogeneous case the propagation is not affected by vertical plane reflections, in the other scenarios field reflections strongly perturb the propagation along z. The influence of these reflections on the field attenuation can be better appreciated in Fig.3, where the electric field intensities along z in the antenna plane ($y = 300\ nm$) for the four investigated scenarios are reported. The fields have been normalized in order to have the same intensity (0 dB) in the far field

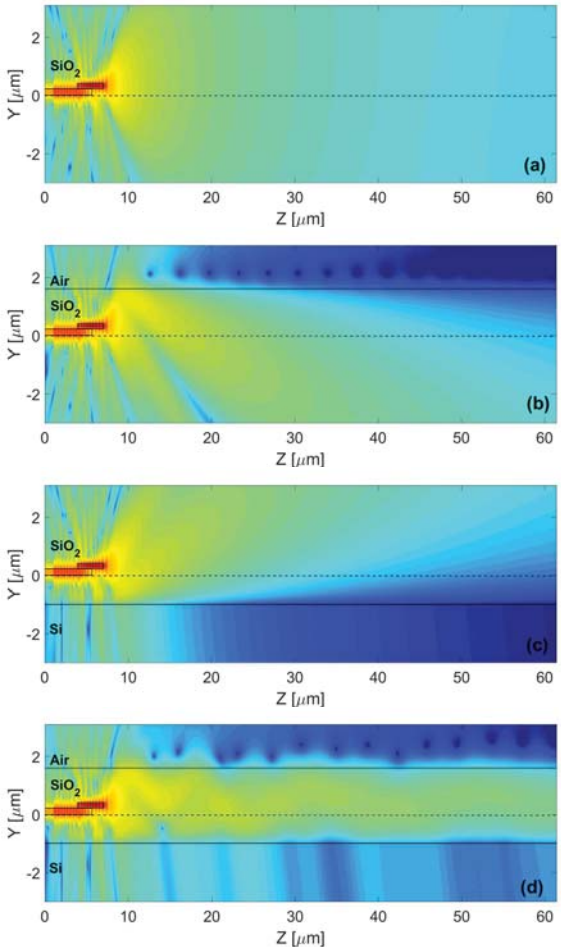

Fig. 2: Patterns (in logarithmic scale) of the electric field intensity $|\mathrm{E}|^2$ in the YZ vertical plane for: (a) homogeneous medium, (b) Air-SiO_2 layers, (c) SiO_2-Si layers, and (d) Air-SiO_2-Si layers. In these simulations, only the transmitting antenna is considered in the simulated scenarios. The wavelength is $\lambda = 1.55\ \mu m$.

region (25 μm from the antenna). In Fig.3, the blue continuous curve refers to the propagation in a homogeneous medium (the (a) case of Fig.2). The dot-dashed dark-green curve is for the propagation with air on the top, whereas the black dotted curve is for the propagation with silicon on the bottom layer (the (b) and (c) cases of Fig.2, respectively). Finally, the red dashed curve refers to the propagation with the two interfaces (the (d) case of Fig.2). In the (a) case the attenuation follows the expected regular $1/r^2$ trend (dashed black curve in Fig.3). For the (b) and (c) configurations, the attenuation becomes greater far away from the source following a $1/r^4$ decay (dash-dot black curve in Fig.3). This is due to the destructive interference between the direct and the reflected signal contribution. In the (d) case, on the contrary, the two interfaces create a sort of waveguiding effect, which improves propagation in the desired direction reducing diffraction phenomena. In the case of the three-layered environment (d), the field intensity

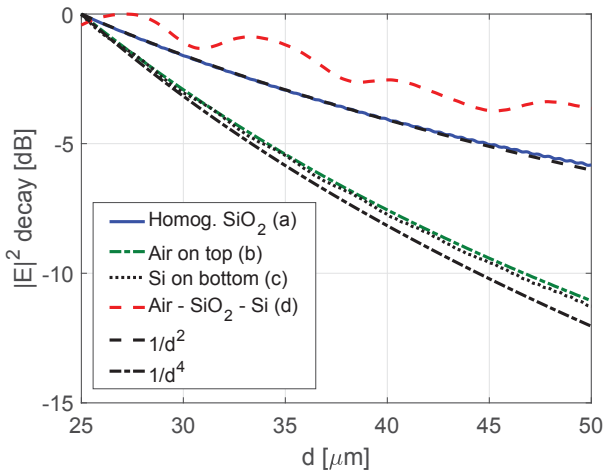

Fig. 3: Decay of the electric field intensity $|\mathrm{E}|^2$ (in dB) along the propagation direction and for different multilayer scenarios. The simulations are performed in the absence of the receiving (Rx) antenna and the wavelength is $\lambda = 1.55\ \mu m$.

is considerably higher than in the other analyzed cases. This leads to obtaining different values of the received power, when a link between two Vivaldi antennas is considered for the four different configurations.

Fig.4 shows the received powers at the output waveguide of the RX antenna as a function of the wavelength and for the four investigated scenarios. The distance between the two antennas is $d = 50\ \mu m$. The received power has been obtained by computing the power flux at the output section for the fundamental mode of the silicon waveguide. In each simulation, an input power $P_{in} = 0\ dBm$ has been considered. As a consequence, the power P_r measured at the output port is directly the power budget of the connection in each scenario. In this figure, the blue continuous curve refers to a link in a homogeneous medium (the (a) case of Fig.2). The dot-dashed dark-green curve is for a link in a scenario with air on the top, whereas the black dotted curve is for a link in the configuration with silicon interface on the bottom layer (the (b) and (c) cases of Fig.2, respectively). Finally, the red dashed curve refers to a wireless link with the two interfaces (the (d) case of Fig.2). At the wavelength of $\lambda = 1.55\ \mu m$, the link in the scenario with a double interface (the (d) case) shows an increase of the received power of $10\ dB$ with respect to the wireless link in a homogeneous environment (the (a) scenario). For the other two configurations, when the interface is with air on the top (scenario (b)), the received power is $P_r = -40\ dBm$, with a reduction of $4\ dB$ with respect to the propagation in a homogeneous medium. The worst case is for the propagation with silicon on the bottom (the (c) configuration), where the reduction of the received power with respect to the (a) case is of about $9\ dB$.

This is also confirmed by the plots of Fig.5, where the field intensity $|\mathrm{E}|^2$ in the YZ vertical plane and for the different investigated configurations is reported. The wavelength is $\lambda =$

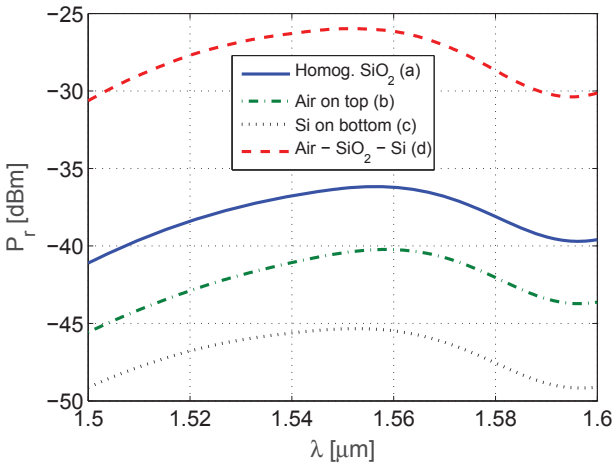

Fig. 4: Received power P_r (in dBm) at the output section of the receiving antenna as a function of wavelength and for the different investigated scenarios.

$1.55\ \mu m$. As it can be noticed, the field confinement of the two interfaces (the (d) scenario) is beneficial for the link. On the contrary, reflections and power leakage of the (b) and (c) scenarios weaken the field at the receiver, with consequent attenuation of the detected power.

IV. Conclusion

In this paper we have investigated the performance of an optical wireless link for Optical Wireless Network on Chip applications in different scenarios. For the link, Vivaldi antennas coupled to silicon waveguides through hybrid Si-plasmonic couplers have been considered. Point-to-point links in multilayered environments have been considered and 3D-FDTD simulations have been performed. Results show that the technology can strongly influence the link properties and cannot be ignored when designing the chip. For example, the presence of a double interface induces an increase of the received power of about $10\ dB$ with respect to the propagation in a homogeneous medium. This phenomenon is due to multiple reflections at the interfaces, that tend to confine the electromagnetic field in the central SiO_2 layer. On the contrary, the presence of a single interface, either on the top or on the bottom side of the link, causes a reduction of the link performance, with an attenuation of the received power with respect to the case of a link in homogeneous environment. The proposed results, obtained via three-dimensional fullwave simulations in a realistic environment, can be a reference for the development of propagation models and ray-tracing algorithms. Once validated with numerical methods ray tracing algorithms can be used to speed up simulations and to investigate wireless channel characteristics also in complex scenarios (presence of cores or waveguides between the transmitter and receiver, broadcast link, etc.).

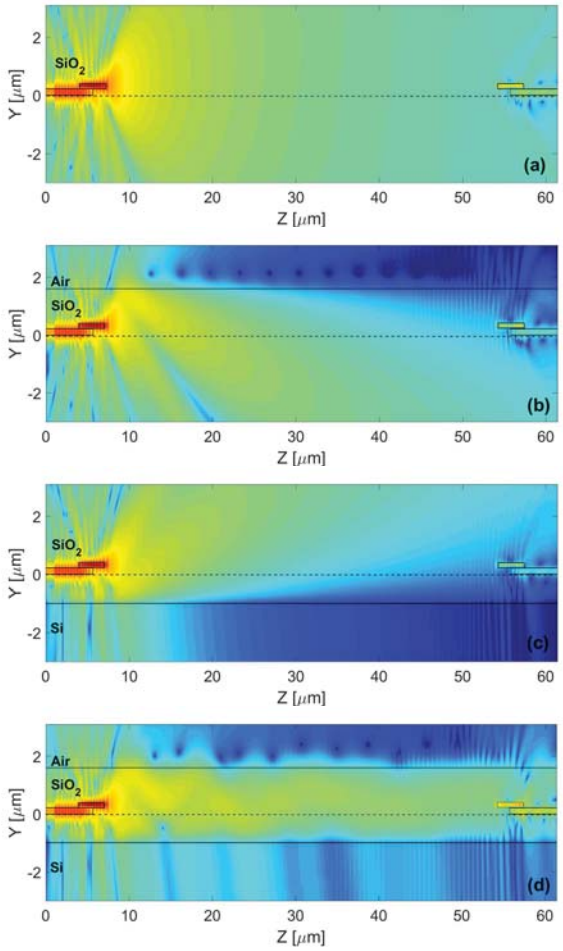

Fig. 5: Patterns (in logarithmic scale) of the electric field intensity $|\mathrm{E}|^2$ in the YZ vertical plane for: (a) homogeneous medium, (b) Air-SiO_2 layers, (c) SiO_2-Si layers, and (d) Air-SiO_2-Si layers for an optical link between two Vivaldi antennas. For all the considered scenarios, the link distance is $d = 50\ \mu m$ and the wavelength is $\lambda = 1.55\ \mu m$.

Acknowledgment

This research was supported by MIUR through the PRIN 2015 "Wireless Networks through on-chip Optical Technology - WiNOT" Project and by Apulia region project "Regional laboratory for synthesis and characterization of new organic and nanostructured materials for electronics, photonics, and advanced technologies". Gaetano Bellanca acknowledges support from "Bando per l'acquisizione di strumenti per la ricerca di Ateneo - Anno 2015" of the University of Ferrara.

References

[1] L. Benini and G. D. Micheli, "Networks on chips: a new SoC paradigm," Computer **35**(1), 70–78 (2002).
[2] A. Shacham, K. Bergman and L.P. Carloni, "Photonic networks-on-chip for future generations of chip multiprocessors," IEEE Trans. Comput. **57**(9), 1246–1260 (2008).
[3] D. B. Miller, "Device requirements for optical interconnects to silicon chips," Proc. IEEE **97**(7), 1166–1185 (2009).

[4] A. Biberman and K. Bergman, "Optical interconnection networks for high-performance computing systems," Rep. Prog. Phys. **75**(4), 046402 (2012).
[5] F. Gambini, S. Faralli, P. Pintus, N. Andriolli and I. Cerutti, "BER evaluation of a low-crosstalk silicon integrated multi-microring network-on-chip," Opt. Express **23**(13), 17169–17178, (2015).
[6] M. Ortin-Obon, M. Tala, L. Ramini, V. Vinals-Yufera and D. Bertozzi, "Contrasting laser power requirements of wavelength-routed optical NoC topologies subject to the floorplanning, placement and routing constraints of a 3D-stacked system," IEEE Transactions Very Large Scale Integr. (VLSI) Syst. (posted 28 March 2017, in press).
[7] C. Garcia-Meca, S. Lechago, A. Brimont, A. Gariol, S. Mas, L. Sánchez, L. Bellieres, N. S. Losilla and J. Martí, "On-chip wireless silicon photonics: from reconfigurable interconnects to lab-on-chip devices," Light: Science & Applications **6**, (2017).
[8] A. Alù and N. Engheta, "Wireless at the nanoscale: optical interconnects using matched nanoantennas," **104**, 213902 (2010).
[9] Y. Yang, Q. Li and M. Qiu, "Broadband nanophotonic wireless links and networks using on-chip integrated plasmonic antennas," Sci. Rep. **6**, 19490 (2016).
[10] J. M. Merlo, N.T. Nesbitt, Y.M. Calm, A.H. Rose, L. D'Imperio, C. Yang, J.R. Naughton, M.J. Burns K. Kempa and M.J. Naughton, "Wireless communication system via nanoscale plasmonic antennas," Sci. Rep. **6**, 31710 (2016).
[11] D. M. Solís, J. M. Taboada, F. Obelleiro and L. Landesa, "Optimization of an optical wireless nanolink using directive nanoantennas," Opt. Express **21**(2), 2369–2377 (2013).
[12] G. Magno, A. Ecarnot, C. Pin, V. Yam, P. Gogol, R. Mgy, B. Cluzel, B. Dagens, " Integrated plasmonic nanotweezers for nanoparticle manipulation" Optics Letters, 41 (16), pp. 3679-3682, (2016).
[13] M. Fvrier, P. Gogol, A. Aassime, R.t Mgy, C. Delacour, A. Chelnokov, A. Apuzzo, S. Blaize, J.. Lourtioz, and B. Dagens, "Giant Coupling Effect between Metal Nanoparticle Chain and Optical Waveguide", Nano Letters 12 (2), 1032-1037, (2012).
[14] L. Yousefi and A. C. Foster, "Waveguide-fed optical hybrid plasmonic patch nano-antenna," Opt. Express **20**(16), 18326-18335 (2012).
[15] Y. Yang, D. Zhao, H. Gong, Q. Li, and M. Qiu, "Plasmonic sectoral horn nanoantennas," Opt. Lett. **39**(11), 3204–3207 (2014).
[16] M. Saad-Bin-Alam, I. Khalil, A. Rahman and A. M. Chowdhury, "Hybrid plasmonic waveguide fed broadband nanoantenna for nanophotonic applications," IEEE Photon. Technol. Lett. **27**(10), 1092–1095 (2015).
[17] G. Bellanca, G.Calò, A. E. Kaplan, P. Bassi, and V. Petruzzelli, "Integrated Vivaldi plasmonic antenna for wireless on-chip optical communications," Opt. Express 25, 16214-16227 (2017)
[18] M. Nafari, L. Feng, and J. M. Jornet, "On-Chip Wireless Optical Channel Modeling for Massive Multi-Core Computing Architectures," 2017 IEEE Wireless Communications and Networking Conference (WCNC), San Francisco, CA, 2017, pp. 1-6.
[19] Lumerical Solutions, Inc. http://www.lumerical.com/tcad-products/fdtd/
[20] A. Yariv, Coupled-mode theory for guided-wave optics, IEEE J. QuantumElectron., QE-9 (9), 919933 (1973).
[21] G. Calò, A. D'Orazio, V. Petruzzelli, Broadband Mach-Zehnder Switch for Photonic Networks on Chip, J. Lightw. Technol. 30, 944-952 (2012).
[22] COMSOL Multiphysics, http://www.comsol.com/